In situ Synthesis of Metal Nanoparticle Embedded Free Standing Multifunctional PDMS Films

Anubha Goyal, Ashavani Kumar,* Prabir K. Patra, Shaily Mahendra, Salomeh Tabatabaei, Pedro J. J. Alvarez, George John, Pulickel M. Ajayan*

We demonstrate a simple one-step method for synthesizing noble metal nanoparticle embedded free standing polydimethylsiloxane (PDMS) composite films. The process involves preparing a homogenous mixture of metal salt (silver, gold and platinum), silicone elastomer and the curing agent (hardener) followed by curing. During the curing process, the hardener crosslinks the elastomer and simultaneously reduces the metal salt to form nanoparticles. This in situ method avoids the use of any external reducing agent/stabilizing agent and leads to a uniform distribution of nanoparticles in the PDMS matrix. The films were characterized using UV-Vis spectroscopy, transmission electron microscopy and X-ray photoemission spectroscopy. The nanoparticle-PDMS films have a higher Young's modulus than pure PDMS films and also show enhanced antibacterial properties. The metal nanoparticle-PDMS films could be used for a number of applications such as for catalysis, optical and biomedical devices and gas separation membranes.

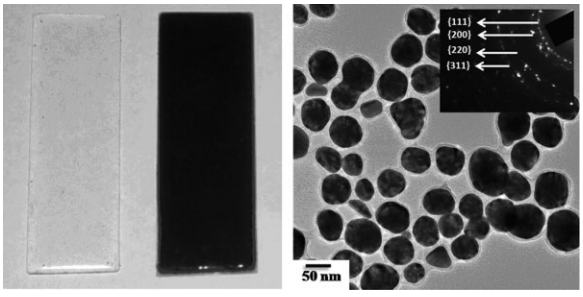

Nanocomposites of inorganic materials in polymer matrices have attracted a great deal of attention because of their wide applications as biosensors,[1] optical devices,[2] micromechanical devices,[3] and advanced catalytic membranes.[4] For the synthesis of nanocomposites, different approaches have been developed such as the incorporation of pre-made nanoparticles into a polymer matrix with the use of a common blending solvent or by reduction of metal salt dispersed in polymeric matrix using an external reducing agent.[5] Nanoparticles can also be embedded in polymers using physical and chemical vapor deposition, ion-implantation and sol–gel synthesis routes.[6–8] Using these approaches, various metal nanoparticle-polymer composites have been synthesized including gold-poly(9,9-dioctylfluorene) for light emitting diodes[5] and iron-poly(methyl methacrylate) for electromagnetic applications.[9] Gao et al. have used palladium-containing hollow polymeric fibers of cellulose acetate, polysulfone, and polyacrylonitrile as catalytic membrane reactors for selective hydrogenation of conjugated dienes.[10]

Polydimethylsiloxane (PDMS) elastomer is of particular interest due to its many useful properties such as high flexibility, ease of molding, low cost, non-toxic nature and

A. Goyal, A. Kumar, P. K. Patra, S. Tabatabaei, P. M. Ajayan
Department of Mechanical Engineering and Materials Science, Rice University, Houston TX 77005
E-mail: ajayan@rice.edu; ak10@rice.edu
S. Mahendra, P. J. J. Alvarez
Department of Civil and Environmental Engineering, Rice University, Houston TX 77005
G. John
Department of Chemistry, City College of the City University of New York, New York, New York 10031

Macromol. Rapid Commun. **2009**, *30*, 1116–1122

DOI: 10.1002/marc.200900174

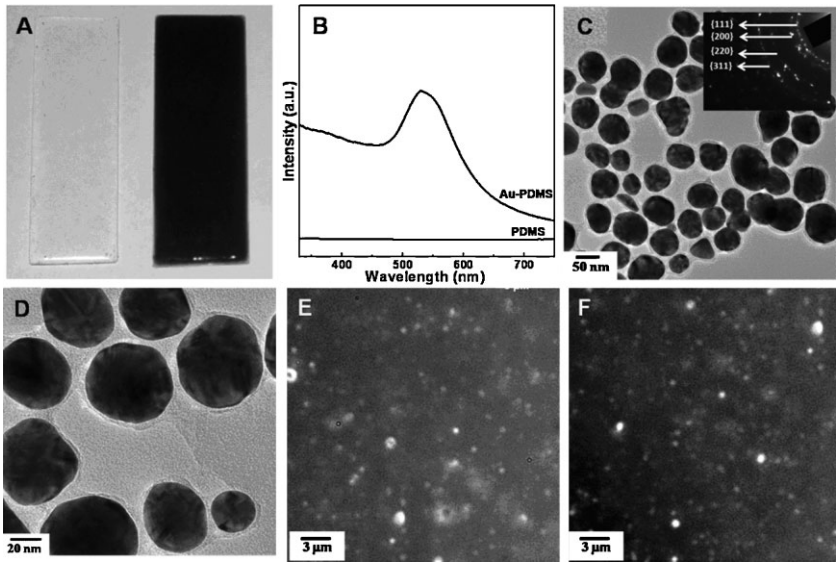

Figure 1. (A) Photograph of pure PDMS and Au-PDMS film showing the color change after the formation of nanoparticles. (B) UV Spectra of the films. (C) and (D) TEM images of the gold nanoparticles formed in PDMS matrix. Inset is the diffraction pattern of the particles. (E) and (F) Optical images of gold nanoparticles embedded in PDMS film.

chemical inertness.[11] It has been used extensively in applications that include microfluidic channels, lubricants, defoaming agents, gas separation membranes and catheters.[12] In spite of its wide use, it has some inherent drawbacks such as mechanical weakness and intolerance to organic solvents.[11] Metal nanoparticle containing film can show enhanced mechanical properties as well as imparts multifunctionality like catalysis and gas separation capability. Therefore, attempts have been made to synthesize metal nanoparticles embedded PDMS films. Gao and co-workers have reported chitosan assisted gold nanoparticle deposition on PDMS surfaces.[13] Chen and co-workers synthesized gold nanoparticle–PDMS composite films by immersing cured PDMS films in gold chloride solution. These films were used for enzyme immobilization and as a chemical reactor. However, their synthesis method involves multiple steps and the nanoparticle concentration is localized to the surface only.[14]

We demonstrate here a simple and inexpensive general process for the synthesis of metal nanoparticle (silver, gold, platinum) embedded PDMS composites. Our method circumvents the need of using pre-formed nanoparticles and gives a bulk dispersion of nanoparticles without requiring any external reducing or stabilizing agent. The process involves adding a metal salt to a mixture of siloxane elastomer and hardener. The hardener performs a dual role of reducing the salt to form nanoparticles and cross-linking the elastomer. This synthesis method leads to a good dispersion of nanoparticles in the polymer matrix. Nanoparticles act as filler and enhance the mechanical properties of PDMS. Young's modulus of nanoparticle containing film is three times higher than that of pure polymer film. Silver containing films show antimicrobial activity making it an ideal candidate for biomedical applications that include implants and urethral catheters. The platinum and gold nanoparticles embedded films can be used for optical and catalytic applications.

Gold, silver, and platinum nanoparticle embedded PDMS film were prepared by dissolving gold chloride, silver benzoate and chloroplatinic acid using appropriate solvent and mixing with elastomer and hardener followed by curing. Figure 1A is the photograph of pure PDMS and gold nanoparticle embedded PDMS film (Au-PDMS). Pure PDMS film is transparent; however, the gold containing film is ruby red which is a characteristic color of gold nanoparticles. Figure 1B is the UV-Visible spectra of these films. Pure PDMS does not show any absorbance in the visible region whereas Au-PDMS has an absorbance centered at ≈530 nm. This absorbance is due to the surface plasmon excitation of gold nanoparticles[14] and confirms the nanoparticle formation. Figure 1C and D are the TEM images of gold nanoparticles which clearly show that the particles are uniform and discrete. The diffraction pattern reveals that they are crystalline in nature. In order to determine the dispersion of nanoparticles in the polymer matrix, optical images (Figure 1E and F) were taken at different regions of the film using a high resolution and high contrast condenser (CytoViva). It is clear from the images that the nanoparticles are uniformly distributed over a large area with out any phase separation. Similarly, platinum nanoparticles were also synthesized in PDMS film and the TEM images are shown in Figure 2. The nanoparticles are irregular and polydispersed in nature

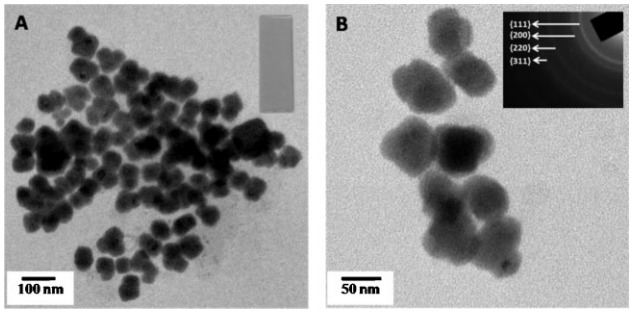

Figure 2. TEM images of the platinum nanoparticles. Inset is the photograph of Pt-PDMS film and the diffraction pattern of platinum nanoparticles.

with an average particle size of 50 nm. The diffraction of platinum nanoparticles (inset of Figure 2B) indicates their fcc crystalline nature.

Silver is well known for its antimicrobial activity and has also been used in polymers for olefin gas separation.[15] Therefore, we extended this method to synthesize silver nanoparticles in PDMS film. Figure 3A is the UV-Vis spectrum and photograph of silver nanoparticle embedded PDMS film. The silver containing film (Ag-PDMS) is yellowish-brown. This characteristic color indicates the formation of silver nanoparticles, which was confirmed by UV-Vis spectroscopy. Ag-PDMS shows a broad absorbance centered at ≈415 nm. The surface plasmon band is broader and shifted to a higher wavelength compared to silver nanoparticles dispersed in a solvent which is in good agreement with the past reports.[16] The nanoparticles were further studied by transmission electron microscopy. Figures 3B and C are the low and high magnification TEM images of a drop casted film of nanoparticles extracted from the Ag-PDMS film. These images indicate that the particles are well defined, discrete and polydispersed. The inset of Figure 3B shows the electron diffraction pattern obtained from the nanoparticles. It is evident from the pattern that the nanoparticles are crystalline and have a fcc structure. Particle size distribution measurement (Figure 3D) yields the size of the particles in the range of 5–20 nm.

In order to understand the chemical interactions of nanoparticles with the PDMS matrix, XPS was performed on a fractured surface of Ag-PDMS film. The general scan spectra of the film at room temperature shows the presence of C1s, Si2p, O1s, and Ag3d core levels with no evidence of impurities. The spectra were background corrected using the Shirley algorithm[17] prior to curve deconvulation. The binding energy of 284.5 eV for adventitious carbon (C1s) was used as the internal standard. Figure 3E shows the Ag3d core level spectrum recorded from the Ag-PDMS film. The spectrum could be resolved into one spin-orbit pairs with the two chemically shifted components, 3d5/2 and 3d3/2 binding energies (BEs) centered at 368.24 and 374.25 eV respectively that correspond to the electron emission from Ag(0)

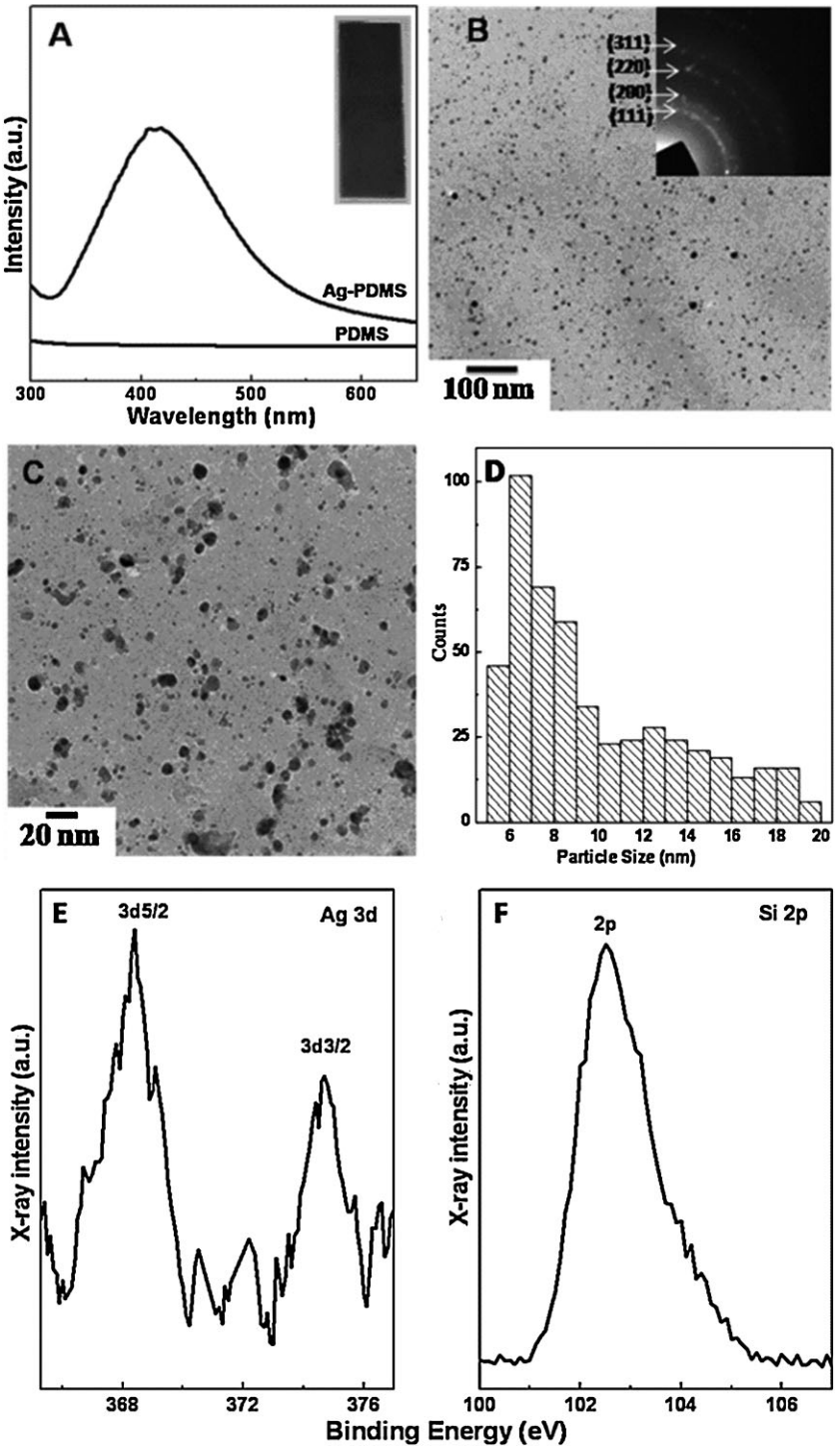

Figure 3. (A) UV-Vis spectrum of PDMS and Ag-PDMS film. Inset is the photograph of Ag-PDMS film. (B) and (C) TEM images of the silver nanoparticles formed in PDMS matrix at different magnification. Inset is the diffraction pattern (D) Particle size distribution obtained from (C) and other images. XPS spectra of Ag-PDMS film showing the binding energy of (E) Ag3d and (F) Si2p core levels.

Macromol. Rapid Commun. **2009**, *30*, 1116–1122

Macromolecular Journals
DOI: 10.1002/marc.200900174

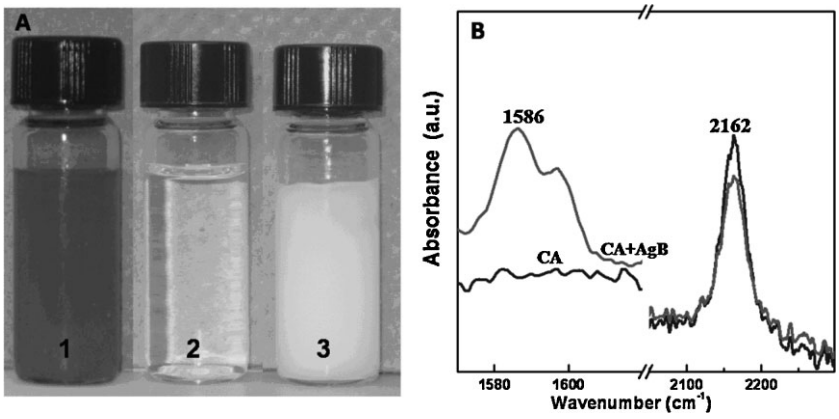

Figure 4. (A) Photographs of vials containing (1) silver benzoate solution with curing agent, (2) pure curing agent and (3) silver benzoate with pure elastomer. (B) FTIR spectra of (1) and (2).

state.[18] The Si2p spectrum recorded from the Ag-PDMS nanoparticles shows a single chemically distinct peak centered at 102.5 eV (Figure 3F) which is in good agreement with the reported value in literature.[19] Absence of any shift in Si2p binding energy in Ag-PDMS as compared to PDMS rules out the possibility of strong chemical interaction between the nanoparticles and the polymer matrix.

To confirm the mechanism of formation of nanoparticles, control experiments were performed wherein silver benzoate solution was separately mixed with pure elastomer and curing agent. The solution with curing agent turned yellowish-brown while the one with pure elastomer showed no color transformation as shown in Figure 4A. Similarly gold and platinum salts were also reduced by curing agent but did now show any reduction with pure elastomer. The control experiments revealed that the curing agent is responsible for the reduction of metal salt. In order to understand the exact mechanism of reduction, FTIR spectra of pure curing agent (CA) and curing agent after formation of nanoparticles (brown colored, CA + AgB) were compared (Figure 4B). The peak at 1 586 cm^{-1} is from carboxylic group present in silver benzoate which is not present in the pure curing agent. The absorbance peak at 2 162 cm^{-1} in both spectra corresponds to the Si–H stretching vibration.[20] The comparison of spectra clearly indicates that the peak intensity of Si–H group gets reduced after formation of silver nanoparticles. This confirms that the Si–H group in curing agent is taking part in the reaction and is responsible for the reduction of metal ions. The Si–H bond gets oxidized to Si–O–Si bond and reduces the metal ions to metal as has been observed in the literature.[14]

Recently, improved mechanical properties of PDMS were achieved by dispersing carbon nanotubes in the polymer.[21] Ci et al. found that the longitudinal modulus and damping capability of carbon nanotube reinforced PDMS matrices were improved by an order of magnitude over pure PDMS. Other materials such as $CaCO_3$, SiO_2 have also been used as fillers in PDMS polymer.[22,23] The effect of filler particle size, shape, and distribution on mechanical properties has widely been studied. Besides this, the filler properties, filler–filler interactions and filler–matrix interactions are also known to play a significant role.[24] It would be interesting to see if in our system also silver nanoparticles affect the mechanical properties of PDMS.

PDMS being a viscoelastic material, dynamic mechanical testing is an appropriate tool for separately examining its elastic and viscous components. Stress-strain curves were recorded for films containing 0.1 weight% silver. Dynamic mechanical analyzer was used in the tension mode at 1 Hz frequency and 0.01 N preload (Figure 5A). The quasi-static Young's modulus was calculated using the slope of the best-fit line to the linear part of the curve extending till 20% strain. Overlay of the stress-strain curves shows that the Young's modulus for the nanoparticle containing films is 1.64 MPa which is approximately three times higher than 0.56 MPa for pure PDMS. The average modulus was found to be 1.7 ± 0.2 MPa for Ag-PDMS and 0.5 ± 0.1 MPa for PDMS. The values for PDMS are comparable to those reported earlier.[25] The increase in modulus for

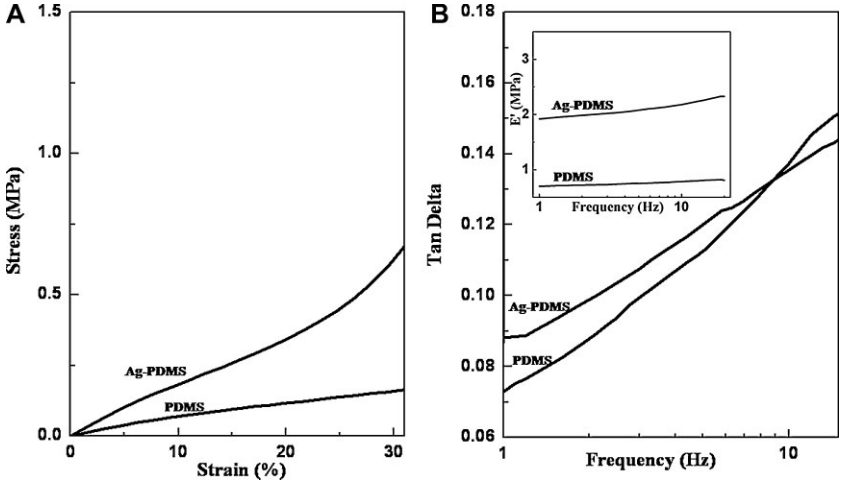

Figure 5. (A) Stress-strain and (B) Tangent delta versus frequency curves for PDMS and Ag-PDMS films. Inset is the comparison of their storage modulus.

Ag-PDMS indicates that the nanoparticles form a good interface with the polymer. This serves to improve load transfer within the nanocomposite network, resulting in a higher modulus.

In order to evaluate differences in the energy damping properties, storage and loss moduli were measured at room temperature as a function of frequency (1–15 Hz) under an oscillatory load. The phase shift, tan delta indicates the damping effectiveness of a material. The dynamic frequency sweep plot (Figure 5B) for the tangent delta values demonstrates that there is no significant difference between the damping capabilities of the two systems. Like any characteristic viscoelastic material, the storage modulus increased with frequency as shown in the inset of Figure 5B. The restraining effect of the inorganic component such as silver on the chain mobility of the PDMS depends on the extent of chain confinement caused by silver nanoparticles at the interface. Owing to very high specific surface area of extremely small silver particles, a good interface is formed between the particles and PDMS which increases the storage modulus reasonably. The friction between relatively less mobile PDMS chains at the interface also increased leading to an increase in the loss modulus also. However, the ratio of the two moduli does not change significantly, thereby keeping tan delta same.

Poor chemical compatibility of PDMS with organic solvents poses a major restriction on its application including PDMS-fabricated microfluidic channel where the studies are restricted to the use of non-wetting polar liquids. It is important to study the behavior of Ag-PDMS films in a range of organic solvents. To quantify the organic solvent tolerance of Ag-PDMS films, pre-weighed films (W_i) were immersed in different solvents at room temperature. The films were weighed at different time intervals (W_o) till no change in weight was seen. This allowed the films to reach equilibrium swelling. The degree of swelling (SD) was calculated based on the difference between the two readings

$$SD(\%) = \left(\frac{W_o - W_i}{W_i}\right) \times 100 \quad (1)$$

Table 1. Percentage degree of swelling.

Solvent	Ag-PDMS Film	PDMS Film
THF	218	175
Toluene	195	132
Methylene Chloride	225	152
Acetone	16	17
Water	0	0

Table 2. Confirmation of antibacterial activity of Ag-PDMS toward *E. coli* and *B. subtilis*. Statistically significant decrease in the number of colony forming units of both strains in the presence of Ag-PDMS indicates its antibacterial activity.

	E. coli (10^4 cfu · mL^{-1})	B. subtilis (10^4 cfu · mL^{-1})
Control culture	3.1 ± 0.3	2.0 ± 0.13
PDMS	3.0 ± 0.3	2.0 ± 0.44
Ag-PDMS	0.66 ± 0.1	0.96 ± 0.12

Comparison of the degree of swelling for Ag-PDMS and PDMS is shown in Table 1 which reveals that in organic medium Ag-PDMS swells more as compared to pure PDMS. However, there is no significant difference in the swelling for polar solvents. The lesser resistance of Ag-PDMS to organic solvents may be due to a lower degree of cross-linking.[25] Some of the curing agent gets consumed in the reduction of the silver salt and hence the available curing agent for cross-linking in Ag-PDMS is less than in pure PDMS which may result in greater swelling.

The presence of silver nanoparticle, makes the PDMS films attractive for biomedical applications[26] and antibacterial coatings[27] due to its inherent antimicrobial properties. The antibacterial activity of Ag-PDMS was studied by incubating *B. subtilis* and *E. coli* bacterial strains with the films. In our study, both (Gram-positive) *B. subtilis* and (Gram-negative) *E. coli* bacteria experienced decreased growth in the presence of Ag-PDMS membranes. Viable plate counts were carried out to distinguish bactericidal from bacteriostatic effects. We found that 80% *E. coli* and 52% *B. subtilis* were inactivated upon 24 h exposure to Ag-PDMS (Table 2). Bacterial growth inhibition and inactivation may be attributed to very low concentrations of silver ions (9 ppb) released from the Ag-PDMS films as measured by ICP. Although exposure to silver ions causes several orders of magnitude reduction in bacterial populations, the amounts of inhibition and inactivation obtained in this study are comparable to those previously reported for products containing silver nanoparticles.[28,29] It is clear that the incorporation of silver nanoparticles confers antibacterial properties to PDMS and extends its use in biomedical applications.

In summary, metal nanoparticle embedded PDMS films were synthesized in situ wherein the hardener was utilized for both reduction and curing. It is a single step process requiring no additional reducing agent. The PDMS films containing silver nanoparticles have a Young's modulus that is greater than that of pure PDMS films by a factor of three, without significantly alteration in damping properties. The presence of silver nanoparticles also make PDMS films antibacterial towards both Gram negative bacteria *Escherichia coli* and Gram positive *Bacillus subtilis*,

Macromol. Rapid Commun. **2009**, *30*, 1116–1122

Macromolecular Journals

DOI: 10.1002/marc.200900174

thus extending their application for antibacterial purposes. Gold and platinum containing films could be used for enzyme immobilization, optical applications, and catalytic activity.

Experimental Part

PDMS elastomer kits (Sylgard 184, Dow Corning) and silver benzoate (Sigma–Aldrich) were used as received. The kit contains the elastomer (PDMS) and the curing agent which is composed of dimethyl, methylhydrogen siloxane, dimethyl siloxane, dimethyl-vinylated, and trimethylated silica, tetramethyl-tetravinyl cyclo-tetrasiloxane, and ethyl benzene. Elastomer (8 g) was mixed thoroughly with the curing agent in the weight ratio of 10:1 and then degassed under vacuum to remove entrapped air bubbles. Silver benzoate (3 ml, 2×10^{-2} M solution in hexane) was added to the polymer and sonicated for 15 min to obtain a homogeneous mixture. Subsequently, the color of the mixture changed to brown. It was then casted on glass slides and cured under vacuum at room temperature. For the preparation of gold and platinum nanoparticles, 10^{-4} M chloroauric acid and 2×10^{-5} M chloroplatinic acid solution in methanol was prepared. Four milliliter of the solution was added to 8 g PDMS dissolved in methylene chloride. The subsequent curing procedure was same as that for silver.

Various techniques such as UV-Vis spectroscopy, transmission electron microscopy (TEM), X-ray photoemission spectroscopy (XPS), optical imaging, and dynamic mechanical testing were used to characterize the product. UV-Vis spectroscopy measurements of the films were performed on a spectrophotometer (Shimadzu UV-3600) operated at a resolution of 1 nm. The size of nanoparticles was determined using transmission electron microscope (JEOL 1230) operated at 120 KV. Optical imaging (CytoViva) was done to determine the particle distribution of the nanoparticles in the matrix. The Olympus BX-41 microscope with 100x magnification oil objective was used to get the images. X-ray photoelectron spectroscopy measurements (PHI Quantera SXM) were carried out using monochromatic Al K_α radiation (1486.6 eV). The beam was incident at an angle of 45° to the sample. Mechanical properties of the nanocomposite films were studied by Dynamic Mechanical Analyzer (TA Instruments Q800). Leaching of silver ions from Ag-PDMS was determined by immersing the films in deionized water (pH 6 ± 0.2) for two months at room temperature, and analyzing the supernatant using an inductively coupled plasma optical emission spectrometer (ICP-OES, PerkinElmer Optima 4300 DV) which has a detection limit of 1 ppb at a wavelength of 328 nm.

For antibacterial studies, the films were carefully sterilized by autoclaving at 121 °C for 30 min and then incubated overnight (16–18 h) with microorganisms. Cultures exposed to pure PDMS without Ag nanoparticles were used as controls. Antimicrobial activity was tested on *Bacillus subtilis* 168 (ATCC 31578; Gram positive) and *Escherichia coli* K12 (ATCC 25404; Gram negative) to evaluate antibacterial efficacy for different bacterial cell wall morphological properties. The strains were grown on Luria-Bertani broth at 37 °C while shaking at 150 rpm, harvested during exponential growth, and resuspended in minimal Davis media for the experiments.[30] Bacterial growth was monitored in the presence of the films. Growth of cells in suspensions was measured in terms of absorbance at 600 nm, and converted to colony forming units ($CFU \cdot mL^{-1}$) using strain specific standard curves. Bacterial mortality was also determined by viable plate counts after 24 h growth.

Acknowledgements: We acknowledge the financial support from *National Science Foundation Division of Materials Research Grant* 0512156. We thank *Jamie Uertz* at CytoViva Inc. for imaging the films.

Received: March 17, 2009; Accepted: March 23, 2009; DOI: 10.1002/marc.200900174

Keywords: antibacterial properties; mechanical properties; nanocomposites; polysiloxanes

[1] M. T. Sulak, O. Gokdogan, A. Gulce, H. Gulce, *Biosens. Bioelect.* **2006**, *21*, 1719.
[2] S. Dire, F. Babonneau, C. Sanchez, J. Livage, *J. Mater. Chem.* **1992**, *2*, 239.
[3] H. Chen, X. Liu, H. Muthuraman, J. H. Zou, J. H. Wang, Q. Dai, Q. Huo, *Adv. Mater.* **2006**, *18*, 2876.
[4] S. S. Ozdemir, M. G. Buonomenna, E. Drioli, *Appl. Catal. a-General* **2006**, *307*, 167.
[5] J. H. Park, Y. T. Lim, O. O. Park, J. K. Kim, J. W. Yu, Y. C. Kim, *Chem. Mater.* **2004**, *16*, 688.
[6] K. S. Giesfeldt, R. M. Connatser, M. A. De Jesus, N. V. Lavrik, P. Dutta, M. J. Sepaniak, *Appl. Spectr.* **2003**, *57*, 1346.
[7] E. W. Kreutz, H. Frerichs, J. Stricker, D. A. Wesner, *Nuclear Instruments & Methods in Physics Research Section B-Beam Interactions with Materials and Atoms* **1995**, *105*, 245.
[8] I. Yoshinaga, N. Yamada, S. Katayama, *J. Sol–Gel Sci. Technol.* **2005**, *35*, 21.
[9] J. L. Wilson, P. Poddar, N. A. Frey, H. Srikanth, K. Mohomed, J. P. Harmon, S. Kotha, J. Wachsmuth, *J. Appl. Phys.* **2004**, *95*, 1439.
[10] H. R. Gao, Y. Xu, S. J. Liao, R. Liu, J. Liu, D. C. Li, D. R. Yu, Y. K. Zhao, Y. H. Fan, *J. Membr. Sci.* **1995**, *106*, 213.
[11] J. N. Lee, C. Park, G. M. Whitesides, *Anal. Chem.* **2003**, *75*, 6544.
[12] F. Abbasi, H. Mirzadeh, A. A. Katbab, *Polym. Int.* **2001**, *50*, 1279.
[13] B. Wang, K. Chen, S. Jiang, F. Reincke, W. J. Tong, D. Y. Wang, C. Y. Gao, *Biomacromolecules* **2006**, *7*, 1203.
[14] Q. Zhang, J. J. Xu, Y. Liu, H. Y. Chen, *Lab on a Chip* **2008**, *8*, 352.
[15] T. Yamaguchi, C. Baertsch, C. A. Koval, R. D. Noble, C. N. Bowman, *J. Membr. Sci.* **1996**, *117*, 151.
[16] B. K. Kuila, A. Garai, A. K. Nandi, *Chem. Mater.* **2007**, *19*, 5443.
[17] D. A. Shirley, *Phys. Rev. B* **1972**, *5*, 4709.
[18] A. Kumar, H. Joshi, R. Pasricha, A. B. Mandale, M. Sastry, *J. Coll. Inter. Sci.* **2003**, *264*, 396.
[19] A. Dane, U. K. Demirok, A. Aydinli, S. Suzer, *J. Phys. Chem. B* **2006**, *110*, 1137.
[20] W. F. Maddams, *Spectroc. Acta Pt. A-Molec. Biomolec. Spectr.* **1994**, *50*, 1967.

[21] L. Ci, J. Suhr, V. Pushparaj, X. Zhang, P. M. Ajayan, *Nano Lett.* **2008**, *8*, 2762.
[22] T. Kaully, A. Siegmann, D. Shacham, *Polym. Compos.* **2008**, *29*, 396.
[23] R. H. Gee, R. S. Maxwell, B. Balazs, *Polymer* **2004**, *45*, 3885.
[24] D. Ciprari, K. Jacob, R. Tannenbaum, *Macromolecules* **2006**, *39*, 6565.
[25] N. Stafie, D. F. Stamatialis, M. Wessling, *Sep. Purif. Technol.* **2005**, *45*, 220.
[26] R. M. Slawson, M. I. Vandyke, H. Lee, J. T. Trevors, *Plasmid* **1992**, *27*, 72.
[27] A. Kumar, P. K. Vemula, P. M. Ajayan, G. John, *Nat. Mater.* **2008**, *7*, 236.
[28] O. Choi, K. K. Deng, N. J. Kim, L. Ross, R. Y. Surampalli, Z. Q. Hu, *Water Res.* **2008**, *42*, 3066.
[29] S. K. Gogoi, P. Gopinath, A. Paul, A. Ramesh, S. S. Ghosh, A. Chattopadhyay, *Langmuir* **2006**, *22*, 9322.
[30] S. Mahendra, H. Zhu, V. L. Colvin, P. J. J. Alvarez, *Environ. Sci. Technol.* **2008**, *42*, 9424.

Macromolecular Journals
DOI: 10.1002/marc.200900174